Cytoplasmic dynein regulates the subcellular distribution of mitochondria by controlling the recruitment of the fission factor dynamin-related protein-1

Aniko Varadi[1,*], Linda I. Johnson-Cadwell[1], Vincenzo Cirulli[2], Yisang Yoon[3], Victoria J. Allan[4] and Guy A. Rutter[1,‡]

[1]Henry Wellcome Laboratories for Integrated Cell Signalling and Department of Biochemistry, School of Medical Sciences, University of Bristol, University Walk, Bristol, BS8 1TD, UK
[2]The Whittier Institute for Diabetes, Laboratory of Developmental Biology, University of California San Diego, La Jolla, CA 92037, USA
[3]Center for Basic Research in Digestive Diseases and Department of Biochemistry and Molecular Biology, Mayo Clinic and Foundation, Rochester, MN 55905, USA
[4]School of Biological Sciences, University of Manchester, 2.205 Stopford Building, Oxford Road, Manchester M13 9PT, UK
*Present address: Centre for Research in Biomedicine, Bristol Genomics Institute, Faculty of Applied Sciences, University of West of England, Bristol, BS16 1QY, UK
‡Author for correspondence (e-mail: g.a.rutter@bris.ac.uk)

Accepted 29 April 2004
Journal of Cell Science 117, 4389-4400 Published by The Company of Biologists 2004
doi:10.1242/jcs.01299

Summary

While the subcellular organisation of mitochondria is likely to influence many aspects of cell physiology, its molecular control is poorly understood. Here, we have investigated the role of the retrograde motor protein complex, dynein-dynactin, in mitochondrial localisation and morphology. Disruption of dynein function, achieved in HeLa cells either by over-expressing the dynactin subunit, dynamitin (p50), or by microinjection of an anti-dynein intermediate chain antibody, resulted in (a) the redistribution of mitochondria to the nuclear periphery, and (b) the formation of long and highly branched mitochondrial structures. Suggesting that an alteration in the balance between mitochondrial fission and fusion may be involved in both of these changes, overexpression of p50 induced the translocation of the fission factor dynamin-related protein (Drp1) from mitochondrial membranes to the cytosol and microsomes. Moreover, a dominant-negative-acting form of Drp1 mimicked the effects of p50 on mitochondrial morphology, while wild-type Drp1 almost completely restored normal mitochondrial distribution in p50 over-expressing cells. Thus, the dynein/dynactin complex plays an unexpected role in the regulation of mitochondrial morphology in living cells, by controlling the recruitment of Drp1 to these organelles.

Key words: Cytoplasmic dynein, Mitochondria, Motor proteins, Fission

Introduction

Mitochondria are vital determinants of both the life and death of cells (Newmeyer and Ferguson-Miller, 2003). Thus, changes in mitochondrial morphology, and the spatial interaction of these organelles with other intracellular structures, seem likely to affect several aspects of cell physiology, including calcium homeostasis (Rutter and Rizzuto, 2000) and the regulation of apoptosis (Karbowski and Youle, 2003). However, knowledge of the mechanisms that control mitochondrial movement and dispersal within the cell remains fragmentary.

Mitochondria appear to adopt a variety of different shapes in living cells, ranging from multiple small compartments (Collins and Bootman, 2003; Collins et al., 2002; Park et al., 2001) to elaborate tubular networks (Rizzuto et al., 1993; Rutter and Rizzuto, 2000; Legros et al., 2002). Suggesting an important role for the cytoskeleton in maintaining their intracellular distribution (Allan and Schroer, 1999), mitochondria interact with microfilaments, intermediate filaments and microtubules (Rappaport et al., 1998; Yaffe, 1999; Karbowski et al., 2001; Knowles et al., 2002) and isolated mitochondria display both (+) and (–) end-directed movements along microtubules (Morris and Hollenbeck, 1995). Several members of the kinesin superfamily have been proposed to drive the anterograde movement of mitochondria (Hirokawa, 1998). Thus, Kif5b (also called kinesin I or conventional kinesin) (Tanaka et al., 1998) is localised to mitochondria in vivo, and function-blocking antibodies to Kif5b inhibit mitochondrial motility on microtubules in vitro (Nangaku et al., 1994). Similarly, inactivation of Kif5b alters mitochondrial distribution in undifferentiated extra-embryonic cells from mice (Tanaka et al., 1998), in *Xenopus laevis* oocytes (Heald et al., 1996) and in mammalian fibroblasts (Krylyshkina et al., 2002; Varadi et al., 2002). By contrast, the identity of the (–) end motor(s) involved is uncertain.

Very recent studies have revealed the identity of some of the principal components of the mitochondrial fission/fusion machinery (Karbowski and Youle, 2003). A member of the dynamin family of GTPases, dynamin-related protein (Drp1, also known as DVLP, DLP1 or Dymple) has been shown to be involved in mitochondrial fission in both yeast and mammals

(Karbowski and Youle, 2003). Thus, expression of a dominant negative mutant of Drp1 results in the formation of highly interconnected, fused mitochondria (Smirnova et al., 1998; Smirnova et al., 2001; Yoon et al., 2001; Pitts et al., 1999).

Here, we have sought to determine the role of the dynein/dynactin complex in the retrograde movement of mitochondria. Unexpectedly, we show that disruption of dynein function in HeLa cells leads to the retreat of mitochondria from the cell periphery towards the nucleus, and the formation of long, interconnected mitochondria. This retrograde movement is associated with a large decrease in the association of Drp1 with mitochondria, and is reversed by overexpression of wild-type Drp1. Moreover, we also show that Drp1 interacts with the dynactin complex and provide evidence that this controls its recruitment to the mitochondrial outer membrane.

Materials and Methods

Materials

cDNAs encoding dynamitin, p50 and p50-enhanced green fluorescent protein (EGFP) (Valetti et al., 1999) were kindly provided by Trina Schroer (Johns Hopkins University, Baltimore) and Vladimir Gelfand (Urbana, Illinois), respectively. Plasmid encoding α-tubulin.EGFP was from David Stephens (University of Bristol, UK). Cell culture reagents were from GibcoBRL (Life Science Research, Paisley, UK) and all molecular biologicals from Roche Diagnostics (Lewes, UK). Electron microscopy (EM) grade paraformaldehyde, glutaraldehyde and sodium cacodylate trihydrate were purchased from Electron Microscopy Sciences (Fort Washington, PA). Alexa Fluor goat anti-rabbit or anti-mouse 488 and 568 secondary antibodies, MitoTrackerRed™ and Oregon Green 488 BAPTA-1 dextran were from Molecular Probes (Eugene, USA). Mouse monoclonal anti-α-tubulin and anti-dynein (Clones 70.1 and 74.1) antibodies and Annexin V-CY3 Apoptosis Detection Kit were obtained from Sigma (Poole, UK). Monoclonal anti-dynamitin p50 was purchased from BD Biosciences (Oxford, UK). Rabbit anti-human Drp1 polyclonal antibody was from AMS Biotechnology (Abingdon Oxon, UK). Mouse monoclonal *trans*-golgi network protein 38 (TGN38) and mouse monoclonal anti-human lysosome-associated membrane protein-1 (LAMP-1) specific antibodies were kindly provided by G. Banting (University of Bristol, UK) (Lee and Banting, 2002).

Cell culture

HeLa cells were cultured in Dulbecco's modified Eagle's medium (DMEM) tissue-culture medium supplemented with 10% (v/v) foetal calf serum (FCS) penicillin (100 units ml^{-1}), streptomycin (0.1 mg ml^{-1}) and L-glutamine (2 mM) at 37°C in an atmosphere of humidified air (95%) and CO_2 (5%) as described previously (Molnar et al., 1995).

Plasmids

A plasmid encoding mitochondrially targeted *Discoidium* red fluorescent protein (mito.DsRed) was generated as described earlier (Varadi et al., 2002).

Live cell imaging immunocytochemistry

Cells were co-transfected with 1 μg of plasmids encoding mito.DsRed and p50, p50.EGFP, or empty vectors (pcDNA3 or pAdTrack-CMV, the latter encodes EGFP) (He et al., 1998), using 10 μg ml^{-1} Lipofectamine in Optimem I™ medium (GibcoBRL, Life Science Research, Paisley, UK) for 4 hours. Alternatively, mitochondria were visualised in p50.EGFP-expressing live cells by staining with 100 nM MitoTrackerRed™ dye in growth medium for 30 minutes at 37°C. Immunocytochemistry was performed as described earlier (Varadi and Rutter, 2002). Images were captured on a Leica TCS-NT confocal laser-scanning microscope attached to a DM IRBE™ epifluorescence microscope using a ×63 PL Apo 1.4 NA oil-immersion objective (Leica, Heidelberg, Germany) or on an Ultra*VIEW*™ live cell confocal imaging system (PerkinElmer Life Sciences, Boston, MA). For live imaging, cells were imaged on the Ultra*VIEW*™ confocal microscope at 2 Hz for 100 seconds (200 frames in total) in Krebs-Ringer-Hepes-Bicarbonate (KRH) buffer comprising 140 mM NaCl, 3.6 mM KCl, 0.5 mM NaH_2PO_4, 0.5 mM $MgSO_4$, 2.0 mM $NaHCO_3$, 16-30 mM glucose, 10 mM Hepes (pH 7.4) and 1.0 mM $CaCl_2$ equilibrated with O_2/CO_2 (95:5, v/v) at 37°C.

Detection of dynein and dynactin subunits on mitochondrial fractions

To detect dynein and the dynactin subunits (p50 and p150^{Glued}) associated with mitochondria, a heavy mitochondrial fraction was obtained that contained predominantly mitochondria with insignificant amounts of contaminants (e.g. lysosomes, peroxisomes, Golgi membranes). HeLa cells were scraped into 500 μl of a buffer containing 0.2 M mannitol, 50 mM sucrose, 1 mM EDTA, 20 mM HEPES-KOH (pH 7.4) homogenisation medium containing 1 μM phenylmethylsulfonyl fluoride (PMSF), 5 μg ml^{-1} aprotinin, and 5 μg ml^{-1} leupeptin and homogenised with a ball bearing homogeniser (25 strokes) on ice before centrifugation at 1000 ***g*** for 10 minutes at 4°C. The resulting low-speed pellet, which contained nuclei and unbroken cells, was discarded. The post-nuclear supernatant (PNSN) was further centrifuged at 3000 ***g*** for 10 minutes at 4°C and the resulting heavy-mitochondrial pellet (HMP) was resuspended in 25 μl homogenisation medium. Equal amounts of protein (3 μg per lane) from the mitochondrial pellet (HMP), post-mitochondrial supernatant (HMSN) and post-nuclear supernatant (PNSN) were separated on a 9% (w/v) polyacrylamide gel then blotted onto Immobilon-P transfer membrane and probed with monoclonal anti-p50, anti-p150^{Glued} and ant-dynein antibodies. The blots were scanned and quantified with NIH ImageJ software (http://rsb.info.nih.gov/ij/). The amount of Drp1 in each subcellular fraction was estimated from the band intensity and the total amount of protein in each fraction.

Analysis of Drp1 association with mitochondria

HeLa cells (at ~75% confluency) in 75 cm^3 culture flasks were transfected with 50 μg plasmid DNA encoding p50.EGFP or empty vector (pAdTrack-CMV) using 50 μg ml^{-1} lipofectamine in Optimem I™ medium (GibcoBRL, Life Science Research, Paisley, UK) for 4 hours. After overnight culture, the transfection efficiency was ⩾75%. Cells were scraped into 750 μl homogenisation medium (0.3 M sucrose, 10 mM Mes K^+, 1 mM K_2EGTA, 1 mM $MgSO_4$, pH 6.5, 1 mM dithiothreitol, 1 μM phenylmethylsulfonyl fluoride (PMSF), 5 μg ml^{-1} aprotinin, and 5 μg ml^{-1} leupeptin) and then homogenised with a ball bearing homogeniser (25 strokes) on ice before centrifugation at 1000 ***g*** for 10 minutes at 4°C. The resulting low-speed pellet, which contained nuclei and unbroken cells, was discarded. The post-nuclear supernatant was further centrifuged at 10,000 ***g*** for 20 minutes at 4°C and the resulting mitochondrial pellet containing both heavy and light mitochondrial fractions was resuspended in 25 μl homogenisation medium. The post-mitochondrial supernatant was further centrifuged at 100,000 ***g*** for 2 hours to obtain microsomal pellet (MP). Equal amounts of protein (26 μg per lane) from the mitochondrial pellet (Mit.P), post-mitochondrial supernatant (PMSN), microsomal pellet (MP) and post-nuclear supernatant (PNSN) were separated on a 9% (w/v) polyacrylamide gel then blotted onto Immobilon-P transfer membrane and probed with a polyclonal anti-human Drp1 antibody. The blots were scanned and quantified with NIH ImageJ software (http://rsb.info.nih.gov/ij/).

Analysis of p150^{Glued} and kinesin I interaction by immunoprecipitation

HeLa cells were lysed in IMB50 containing 50 mM imidazole, pH

7.4, 1 mM EGTA, 0.5 mM EDTA, 5 mM magnesium acetate, 175 mM sucrose, 1 mM DTT, 1 μM PMSF, 5 μg ml^{-1} aprotinin, and 5 μg ml^{-1} leupeptin and centrifuged at 16,000 ***g*** for 10 minutes. Extracts were precleared for 60 minutes with pre-packed protein-A sepharose (Bio-Rad) to remove proteins that would bind nonspecifically. After brief centrifugation, the preadsorbed samples were incubated for 60 minutes at room temperature with 2 μg antibodies pre-bound to 25 μl of prepacked protein-A sepharose. The beads were collected by a brief centrifugation and washed two times with IMB50 and IMB50 containing 250 mM NaCl (Deacon et al., 2003). The following antibodies were used: mouse monoclonal anti-$p150^{Glued}$, mouse monoclonal SUK4, mouse monoclonal dynein intermediate chain (DIC) clone 74.1, mouse monoclonal anti-p50, rabbit polyclonal anti-kinesin light chain and mouse monoclonal anti-GFP (green fluorescent protein).

Analysis of Drp1 and dynactin interaction

HeLa cells were homogenised in (a) 20 mM Tris-HCl (pH 7.5) buffer containing 2 mM $MgCl_2$, 50 mM KCl, 1 mM EGTA, 1 μM PMSF, 5 μg ml^{-1} aprotinin, and 5 μg ml^{-1} leupeptin but no detergent (–NP40 buffer) or in (b) radioimmunoprecipitation lysis buffer (RIPA) containing 150 mM NaCl, 10 mM Tris (pH 7.4), 1% (v/v) Nonidet P40 (NP40), 0.5% (w/v) sodium deoxycholate, 0.1% (w/v) SDS, 1 μM PMSF, 5 μg ml^{-1} aprotinin, and 5 μg ml^{-1} leupeptin (+NP40 buffer). After homogenisation with a ball bearing homogeniser (25 strokes) in the –NP40 buffer cell homogenate was centrifuged at 1,000 ***g*** for 10 minutes at 4°C. The cell lysate obtained in RIPA buffer was centrifuged at 10,000 ***g*** for 10 minutes. Both extracts were precleared for 60 minutes with pre-packed protein-G PLUS Agarose (Santa Cruz) to remove proteins that would bind nonspecifically. After brief centrifugation, the pre-adsorbed samples were incubated overnight at 4°C with 2 μg antibodies pre-bound to 20 μl of prepacked protein-G PLUS Agarose. The beads were collected by a brief centrifugation and washed three times with –NP40 or +NP40 buffer. The following antibodies were used: mouse monoclonal anti-$p150^{Glued}$, mouse monoclonal anti-p50, rabbit polyclonal anti-human Drp1, rabbit preimmun sera and mouse monoclonal anti-GFP.

Measurement of luciferase luminescence

Cells cultured on 13 mm diameter poly-L-lysine-coated coverslips were co-transfected with 0.5 μg plasmid DNA encoding mit.Luc and 1 μg p50 or empty vector (pcDNA3) using Lipofectamine (Promega). For monitoring changes in mitochondrial ATP synthesis, cells were constantly perifused with KRH buffer supplemented with 20 μM luciferin, 0.1 mM pyruvate and 1 mM lactate then challenged with 100 μM histamine (Jouaville et al., 1999).

Microinjection

Mouse anti-dynein monoclonal antibody (Clone 70.1) was dialysed against 2 mM Tris-HCl (pH 8.0) buffer containing 0.2 mM Na^+-EDTA, then microinjected at concentration of 1 mg ml^{-1} together with 1 mg ml^{-1} Oregon Green 488 BAPTA-1 dextran into HeLa cells previously transfected with mito.RsRed.

Electron microscopy

Cells were fixed in 0.1 M sodium cacodylate trihydrate buffer (pH 7.4, at 37°C) containing 2% (w/v) paraformaldehyde, 2.5% (w/v) glutaraldehyde, 3 μM $CaCl_2$ for 4 hours at room temperature. Samples were then post-fixed with osmium tetraoxide (1% (w/v) in H_2O) and counterstained with uranyl acetate (2% (w/v) in H_2O). Following gradual dehydration in ethanol, samples were embedded in Durcupan resin (Sigma Immunochemicals) and polymerized overnight at 60°C and –20 mm Hg, as described (Staubli, 1963). Ultrathin sections (80 nm) were then cut using a 35° angle Diatome diamond knife, and mounted on 300 mesh gold grids (Electron Microscopy Sciences, Fort Washington, PA). Following counterstaining with uranyl acetate (1% (w/v) in H_2O) and Sato lead [1% (w/v) in H_2O] sections were imaged at 80 keV using an electron microscope (1200FX; JEOL, Akashima, Japan).

Statistical analysis

Data are presented as the mean ±s.e.m. for the number of observations given, and statistical significance calculated using Student's *t*-test.

Results

Effects of dynamitin (p50) overexpression on mitochondrial morphology

Expression of mitochondrially targeted DsRed in control (empty vector-transfected) HeLa cells, and acquisition of confocal images, revealed the existence of mitochondria with a variety of structures and lengths (Fig. 1A,a,b; Fig. 2A,a,c). Regions of high apparent mitochondrial connectivity (i.e. a mitochondrial 'reticulum') (Rizzuto et al., 1998) (Fig. 2A,a,c), as well as clearly discrete, individual mitochondria (Fig. 1A, Fig. 2A,a,c) (Collins et al., 2002) were also evident. A large proportion (65-70%, examined in seven cells co-expressing mito.DsRed and α-tubulin.EGFP) of single mitochondria were located along microtubules in living cells (Fig. 1A,a,b) and mitochondria were also apparent at the cell periphery in control cells (Fig. 1A,a,b; 2A,a,c,B).

Cytoplasmic dynein is a multisubunit microtubule motor protein complex that is implicated in the control of a wide variety of cellular processes (Allan and Schroer, 1999). To drive the movement of cargo organelles, dynein requires the accessory factor dynactin (Gill et al., 1991; Burkhardt et al., 1997). Like cytoplasmic dynein, dynactin is a large, multisubunit complex (Holleran et al., 1998) that can be disrupted by overexpression of its dynamitin (p50) subunit (Echeverri et al., 1996; Burkhardt et al., 1997). To detect dynactin subunits and dynein on mitochondria, we prepared a heavy mitochondrial fraction that contained predominantly mitochondrial membranes and was essentially free of the presence of other organelles. p50, $p150^{Glued}$ and dynein were associated with mitochondrial ractions (Fig. 1C) and more than 10% of the total cellular content of each protein was found in the heavy mitochondrial fraction. Whereas depolymerisation of microtubules with nocodazole had relatively little effect on mitochondrial structure (Fig. 1B), overexpression of p50 led to a dramatic relocalisation of the mitochondria towards the nuclear periphery, as assessed using either mitochondrially targeted DsRed (Varadi et al., 2002) (Fig. 2A, e versus a), or the mitochondrial stain, MitoTrackerRed^{TM} (Fig. 2A, g versus c). The effect of p50 on mitochondrial distribution was highly reproducible and was unaffected by fusion of EGFP at the C-terminus of p50 (Fig. 2A, e versus g). Moreover, the severity of mitochondrial redistribution correlated well with the extent of p50 overexpression. Thus, in cells that expressed moderate levels (~50% of median fluorescence) of exogenous p50 (based on fluorescence intensity of EGFP or anti-p50 staining) 43% (66 out of 150 cells) showed a largely interconnected mitochondrial structure that had a tendency to localise some distance from the plasma membrane. By contrast, the majority (116 out of 200 or 58%; data from five independent experiments) of cells with high (~70% median fluorescence) dynamitin levels displayed 'collapsed' mitochondria. Moreover, we observed a similar relocalisation of mitochondria in a metabolically more active cell type MIN6 pancreatic β-cell (data not shown).

Limitations of the above methodology are that: (a) the apparent redistribution of mitochondria may simply reflect a change in the ability of those mitochondria at the cell periphery to accumulate the probes, and (b) that careful analysis of the effect of p50 on mitochondrial morphology was not possible at the resolution of the light microscope due to the high density of mitochondria close to the nucleus (Fig. 2A,e,g). To circumvent both of these problems, we examined changes in mitochondrial morphology by electron microscopy (EM) (Fig. 2B-D). This approach clearly demonstrated that p50 overexpression caused a marked accumulation of mitochondria close to the nucleus, and a complete loss of mitochondria at more remote regions of the cell (Fig. 2, C versus B). Moreover, mitochondria with highly unusual, branched (Fig. 2D and Fig. 3A) and elongated (Fig. 3B) morphology were also evident in p50-transfected cells, but were not observed in control cells. Thus, we consistently observed that ~15% of mitochondria in p50 transfected HeLa exhibited a 'Y' or 'T' shape as opposed to control cells in which such structures were rarely observed (less than 1% of mitochondria). Furthermore, ~10% of mitochondria in p50 transfectants presented an elongated morphology, at times reaching ~12 μm in length, compared with control cells (mitochondria <2.5 μm).

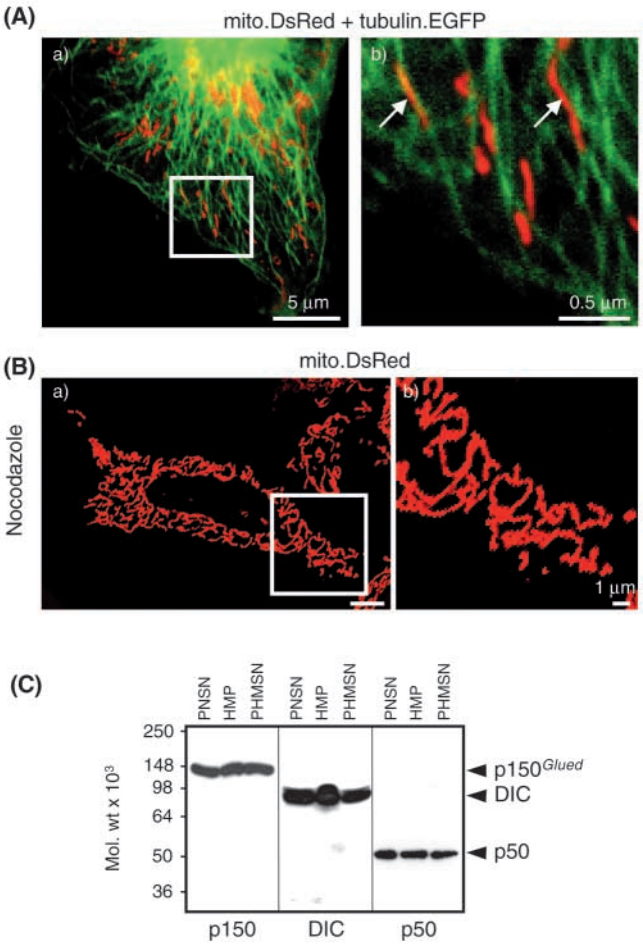

Fig. 1. Mitochondria are partially localised along microtubules in live HeLa cells. (A) Cells were co-transfected with 0.25 μg mito.DsRed and 1 μg α-tubulin.EGFP. Forty-eight hours after transfection cells were imaged on an Ultra*VIEW*™ Live Cell Confocal Imaging system in KRH buffer (see Materials and Methods) at 22°C. The boxed region in a is shown on an expanded scale in b); arrows in b indicate regions of colocalisation. (B) Microtubules were depolymerised with 10 μM nocodazole. The boxed region in a is shown on an expanded scale in b. Bars, 1.0 μm. (C) Dynactin subunits (p50 and p150^{Glued}) and dynein are associated with a mitochondrial fraction. Heavy mitochondrial pellet (HMP) was obtained after spinning the post-nuclear supernatant (PNSN) at 3000 ***g*** for 10 minutes (see Materials and Methods). An equal amount (3 μg) of protein was loaded each lane. The intensity of the protein bands was measured using NIH ImageJ software (http://rsb.info.nih.gov/ij/). PHMSN, post-heavy mitochondrial supernatant; DIC, dynein intermediate chain.

Acute disruption of cytoplasmic dynein activity mimics the effects of p50 overexpression

To confirm that the observed redistribution of the mitochondria induced by p50 overexpression was due directly to inhibition of cytoplasmic dynein, rather than factors, such as cell-cycle blockade (at pro- and meta-phase), or a change in mitochondrial number, we next microinjected a function-blocking antibody (Heald et al., 1996; Burkhardt et al., 1997) against the 74 kDa intermediate chain of cytoplasmic dynein (DIC). Microinjection of anti-DIC induced a clear and rapid (within 2-4 hours) relocalisation of the mitochondria to the nuclear periphery (Fig. 4A,c,d) in a manner closely similar to the effect of p50 overexpression (Fig. 2A,e,g). The effect of anti-DIC was dose-dependent (not shown), and was not mimicked by a control antibody used at the same concentration (Fig. 4Aa,b,B).

p50 overexpression causes an anterograde redistribution of the Golgi complex and endocytic organelles

Given the unexpected effect of p50 on mitochondrial distribution, we next tested the effects of p50.EGFP overexpression on other organelles, whose distribution has been reported to be dynein-dynactin dependent (Burkhardt et al., 1997; Helfand et al., 2002). As anticipated, overexpression of p50 caused fragmentation and redistribution of the Golgi complex (Fig. 4C,a, arrowhead versus control cells, asterisk). This staining pattern was observed in 51% of p50-expressing cells (187/370 cells, three independent experiments). A dramatic redistribution of lysosomes and late endosomes was also revealed in p50-transfected cells with an anti-lysosome-associated membrane protein (LAMP-1) antibody (Lee and Banting, 2002) (Fig. 4C,c). These organelles were shifted away from the cell centre, accumulating at the extreme periphery and processes of the cell (Fig. 4C,c; arrowhead versus control cell, asterisk). However, this phenotype was rare, being observed in ~20% of p50-expressing cells (85/425 cells, three independent experiments).

Over expression of p50 also had relatively minor effects on the distribution of microtubules and microfilaments (not shown). Thus, 51% (153/300 cells, three independent experiments) of control (pAdTrack-CMV transfected) cells had clear MTOC located near the nucleus, which decreased to 35% (122/350 cells, three independent experiments) after transfection with p50. In 85% (424/500, three independent experiments) of control (pAdTrack-CMV expressing) cells, the vimentin network of intermediate filaments extended from the nucleus to the cell periphery, with the majority of vimentin filaments in the perinuclear region. After p50 overexpression,

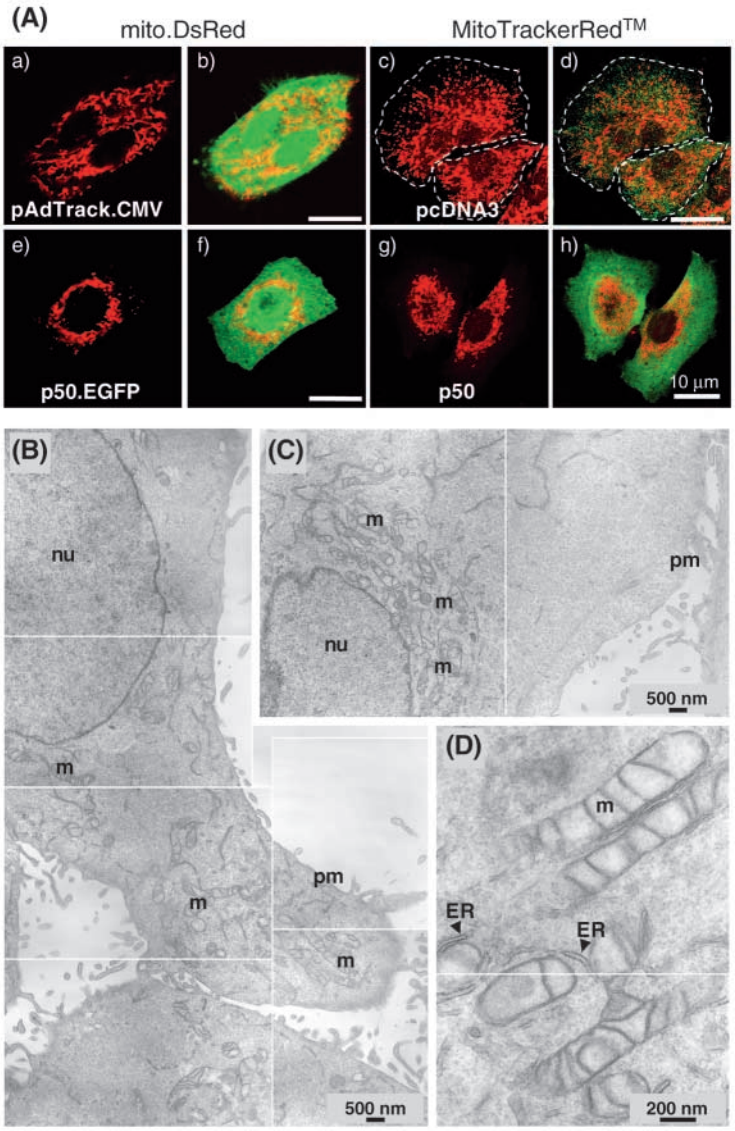

Fig. 2. Overexpression of dynamitin (p50) induces mitochondrial collapse around the nucleus and MTOC. (A) HeLa cells were co-transfected with 0.5 µg mito.DsRed (a,b,e,f) and 1 µg pAdTrack-CMV (empty vector/control) (a,b) or p50.EGFP (e,f). Mitochondria were visualised with MitoTrackerRed™ (c,d,g,h) in cells transfected with either pcDNA3 (empty vector/control) (c,d) or p50.pcDNA3 (g,h). Hatched boundaries in c and d indicate the cell periphery. Twelve hours after transfection, cells were either imaged on a Leica TCS-NT confocal microscope (a,b,e,f) or fixed (c,d,g,h) and were then immunostained with a mouse monoclonal anti-p50 antibody (1:250) and visualised with an Alexa Fluor 488 goat anti-mouse secondary antibody (1:500) before confocal imaging. p50-overexpressing cells were identified by exciting either EGFP or the secondary antibody at 488 nm. DsRed or MitoTrackerRed™ fluorescence was visualised in the same cells by exciting at 568 nm. Typical confocal images of DsRed-labelled mitochondria in control or p50-expressing cells are shown in a and e, MitoTrackerRed™ fluorescence in c and g, composite images b,d,f and h. Note the re-localisation of mitochondria close to the nucleus in p50-expressing cells (e versus a, g versus c). Bars, 10 µm. (B) Reconstruction of adjacent transmission electron microscopic fields showing a (B) control-HeLa cell with randomly distributed mitochondria throughout the cytosol and a (C) p50-transfected HeLa cell with mitochondria redistributed to the perinuclear region within 2-3 µm of the nuclear membrane. Mitochondria are largely absent at the cell periphery. (D) Same section as shown in C at higher magnification. Tight association of mitochondria with the ER is evident. ER, endoplasmic reticulum; m, mitochondria; nu, nucleus; pm, plasma membrane.

there was a clear reduction in vimentin staining in the perinuclear region with intense staining near the cell surface in 27% (53/200 cells, three independent experiments) of p50 over-expressing cells. However, considerable vimentin staining was also still seen throughout the cytoplasm. No detectable effects of p50 overexpression were apparent on the F-actin network (data not shown), overall cell morphology (Figs 2 and 4), or endoplasmic reticulum (ER) distribution (Varadi et al., 2004).

To eliminate the possibility that the p50 overexpression-induced relocalisation of mitochondria may be secondary to changes in the mitochondrial membrane potential ($\Delta\psi_{mit}$) (Ishihara et al., 2003; Legros et al., 2002) we loaded the cells with the positively charged dye tetramethylrhodamine ethyl ester (TMRE) (Ainscow et al., 2000). TMRE fluorescence was 28±3.5 (n=6 cells) and 30±3.1 (n=14 cells) arbitrary units in control and p50-expressing cells, respectively (Fig. 4D). Changes in free mitochondrial ATP concentration in response to histamine, measured using a recombinant targeted luciferase (Jouaville et al., 1999) were also unaffected by p50 overexpression (Varadi et al., 2004). Finally, expression of p50 had no impact on the incidence of apoptosis as assessed by staining phosphatidylserine at the cell surface. Thus, measured at either 24 or 48 hours after transfection, no apparently apoptotic cells were found among the 234 p50-expressing cells that were examined.

Interaction between kinesin I and dynactin

One possible explanation for the above effects of p50 on mitochondrial structure is that disruption of the dynactin complex inhibits both dynein- and kinesin-I-based transport, such that the net localisation of the mitochondria is then determined only by actin-based motility. To test whether kinesin I and dynein interacted via the dynactin complex, as recently shown for kinesin II (Deacon et al., 2002), we performed co-immunoprecipitation of HeLa cell extracts using the protocol described previously (Deacon et al., 2002) with a monoclonal antibody against the p150^{Glued} subunit of the dynactin complex. A very weak protein band corresponding to kinesin I heavy chain (KHC) was observed in the p150^{Glued} immunoprecipitated samples but was absent from control samples (Fig. 5A). The same blots were also probed for a known interaction partner of p150^{Glued}, dynamitin (p50) (Gill et al., 1991). As expected, the anti-p50 antibody revealed a very strong protein band in the immunoprecipitated samples but not in controls (Fig. 5A). In contrast, a monoclonal anti-DIC antibody did not pull down kinesin I light or heavy chain (data not shown) but did immunoprecipitate p150^{Glued}. By contrast, when the immunoprecipitation protocol described previously (Martin et al., 1999) was used, p150^{Glued} did not pull down kinesin I,

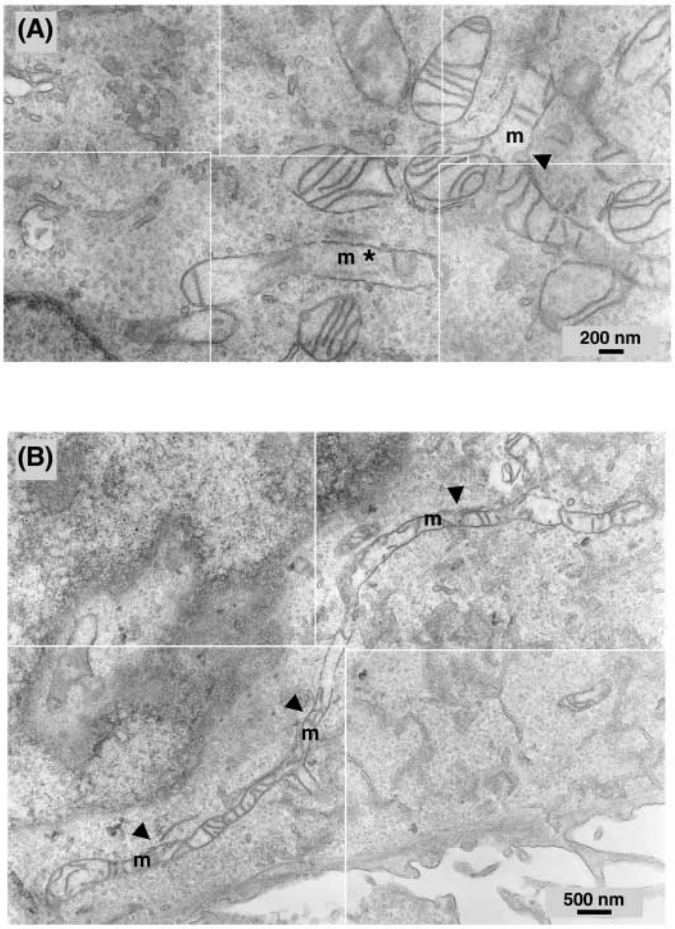

Fig. 3. Overexpression of p50 alters mitochondrial morphology and ultrastructure. Transmission electron micrographs of p50-expressing HeLa cell cross-sections at high magnification show unusually branched (A) or elongated (B) morphology of the mitochondria. Arrowhead in A indicates the branching of mitochondria; Arrowheads in B indicate a single mitochondrion of ~10 μm in length. Notice the dramatic loss of cisternae in the mitochondria marked with an asterisk in A.

presumably as a result of the presence of Triton X-100 in the buffer. Although these results indicate that a small proportion of kinesin I and dynactin may directly interact in HeLa cells, it is apparent that the extent of this interaction is very limited.

To test whether myosin-driven inward movements and microfilaments could instead be responsible for the collapse of mitochondrial structure in p50 over-expressing cells, we depolymerised the microfilaments with latrunculin B. In agreement with the observation that the majority of mitochondria are localised along microtubules (Fig. 1), latrunculin B treatment partially reversed the effects of p50 in 36% of cells examined (9 out of 25 cells, Fig. 5B), while having no evident effect on mitochondrial distribution in control cells. These observations indicate that myosin-driven movements may play some role in the relocalisation of the mitochondria following disruption of the dynein-dynactin complex. We next analysed the effect of p50 overexpression on mitochondrial movements in live cells. Mitochondria were visualised by expression of mito.DsRed and images were taken at 2 Hz on the Ultra*VIEW*^{TM} confocal microscope. Twenty-five mitochondrial regions were selected in ten control cells (Fig. 6A), and in cells with moderate (Fig. 6B) or high (Fig. 6C) p50 expression levels, then movements of mitochondria were analysed off-line. In control cells three main types of mitochondrial movements were observed [see supplemental data Movie 1 and 2 http://jcs.biologists.org/cgi/content/full/117/19/4389/DC1)]. A large proportion of mitochondria (>50%) showed Brownian or thermal motion, ~30% showed a push-forward-retract type of movement (Fig. 6A,b and supplementary material Movie 1) and ~10% showed what appeared to be 'true' active transport on microtubules (Fig. 6A,a, supplementary material Movie 2). This latter movement was not observed following nocodazole treatment (data not shown). At an intermediate level of p50 expression, the mitochondria became more interconnected (Fig. 6B,a,b and supplementary material Movie 3) but collapsed around the nucleus at high p50 expression (Fig. 6C,c and supplemental data Movie 4). Even in cells with collapsed mitochondria, outward movements of individual mitochondria could be observed (Fig. 6C and supplementary material Movie 5). We cannot exclude the possibility that p50 overexpression inhibits motor function to different extent in different regions of the cell a phenomenon that might explain the detection of active movements of mitochondria even at high p50 expression levels. However, inhibition of both kinesin- and dynein-driven movements cannot fully explain the increased interconnectivity of mitochondria in p50 expressing cells because it was not observed after nocodazole treatment (Fig. 1C).

Over expression of p50 alters Drp1 distribution

Over expression of p50 not only induced aggregation of the mitochondria but also altered their morphology (Fig. 2D and Fig. 3A,B). This observation suggested that the dynamic balance between fusion and fission events may be affected when dynein function is inhibited. To test this possibility, we investigated the effect of p50 overexpression on the distribution of the human dynamin-related protein (Drp1), which is required for mitochondrial fission in yeast (Bleazard et al., 1999) and mammalian cells (Smirnova et al., 2001; Yoon et al., 2001). Endogenous Drp1 was associated with numerous punctate, vesicle-like structures in control cells (Fig. 7b,f, and Fig. 8A,a). A large proportion of these Drp1-positive puncta were aligned along microtubules (Fig. 7e-g,II,III). Co-staining of microtubules and Drp1 showed that a proportion of the discrete Drp1-positive puncta were arranged along single microtubules (Fig. 7,III, arrows). Double labelling with mito.DsRed and anti-Drp1 antibody revealed that a fraction of the Drp1-positive puncta localised to mitochondria (Fig. 7a-c,I, arrows). However, the linear arrays of apparent Drp1-positive observed in control cells (Fig. 7b,f and Fig. 8A, a,c, n=57 cells) were replaced by a markedly different, diffuse staining for Drp1 in p50-over-expressing cells (Fig. 8A,b,d, n=23 cells). In accordance with this, subcellular fractionation of HeLa cells revealed that p50 overexpression reduced the amount of Drp1 associated with mitochondria by 55% (Fig. 8C, lanes 'Mito.P'). A large proportion of Drp1 was found in the post-mitochondrial supernatant (93% and 95% in control and p50 cells, respectively; Fig. 8C, lanes 'PMSN') calculated from the intensity of Drp1 bands and protein concentrations in each fraction. In agreement with previously published data

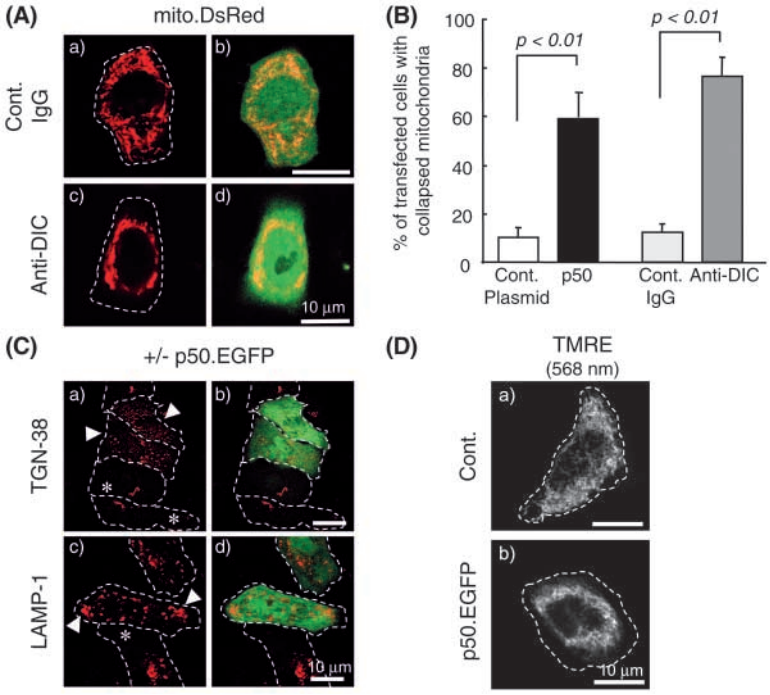

Fig. 4. The effect of p50-overexpression on mitochondrial distribution is mimicked by anti-dynein antibody. (A) Cells were transfected with 0.5 μg mito.DsRed for 16 hours then microinjected together with either 1 mg ml^{-1} control IgG (a,b) or a mouse monoclonal anti-dynein intermediate chain (DIC) antibody (c,d) and 1 mg ml^{-1} Oregon Green BAPTA dextran. Two to four hours after injection, antibody-treated cells were identified by exciting Oregon Green at 488 nm and using fluorescein isothiocyanate filters for fluorescence emission on the Leica confocal microscope. Typical 568 nm in vivo confocal images of mitochondria in control IgG (a) and anti-DIC antibody (c) injected cells; b and d composite images. Bars, 10 μm. (B) The collapsed mitochondria phenotype was scored in cells transfected with p50 or microinjected with the anti-DIC antibody. Data are presented as the number of cells exhibiting this phenotype as a fraction of the total number of cells transfected or microinjected. Two-hundred p50-expressing and ten microinjected cells were analysed in five independent experiments. (C) Effects of p50 overexpression on endocytic organelles. HeLa cells were transiently transfected with p50.EGFP (as described above), and fixed and stained 12 hours later. Immunocytochemistry was performed using a (a,b) monoclonal anti-TGN38 antibody (Lee and Banting, 2002) and a (c,d) monoclonal anti-lysosome-associated membrane protein LAMP-1 antibody (a marker of late endosomes and lysosomes (Ihrke et al., 1998). Fluorescence of an Alexa 568 goat anti-mouse secondary antibody was then visualised in a and c at 568 nm. Intrinsic EGFP fluorescence was visualized at 488 nm in b and d, which are composite images also showing TGN38 and LAMP1 immunostaining, respectively .Arrowheads in a) indicate the position of p50-expressing cells; arrowheads in c) indicate the extreme shift of LAMP-positive late endosomes and lysosomes into the periphery after p50 overexpression. Asterisks indicate control cells. Bars, 10 μm. (D) Overexpression of p50 has no effect on mitochondrial membrane potential ($\Delta\psi_{mit}$). Cells were incubated with 1 μM TMRE for 30 minutes and confocal images were subsequently acquired. Using identical confocal settings, TMRE fluorescence was 28±3.5 (n=6) and 30±3.1 (n=14) arbitrary units in control (a) and p50-expressing (b) cells, respectively. Bars=10 μm (A-E). Hatched boundaries in A, C and D, obtained from an overlay with the transmitted image of the cell, indicate the cell periphery.

(Smirnova et al., 2001) a very small fraction <2% of Drp1 could be pelleted by high-speed centrifugation (Fig. 8C, lanes 'MP'). The intensity of Drp1 in MP was 40% higher in the p50-expressing cells than controls, suggesting that a fraction of Drp1 from mitochondrial membranes relocalised into this fraction. The total amount of Drp1 was not affected significantly by p50 overexpression (Fig. 8C, lanes 'PNSN').

To test whether the effects of p50 on mitochondrial distribution are due to a depletion of the mitochondrial pool of Drp1, we explored the action of introduced Drp1 in cells also over-expressing p50. Co-expression of Drp1 restored, at least in part, the normal distribution of mitochondria in p50 over-expressing cells (Fig. 8B,c, observed in 17/17 cells examined as well as the amount of Drp1 on mitochondrial membranes (Fig. 8D, lanes 'Mito.P'). By contrast, overexpression of a mutant Drp1 ($Drp1^{K38A}$, carrying a point mutation in the GTPase domain) caused a strikingly similar collapsed mitochondrial phenotype to that caused by p50 overexpression (Fig. 8B,d) (Smirnova et al., 1998; Smirnova et al., 2001; Yoon et al., 1998).

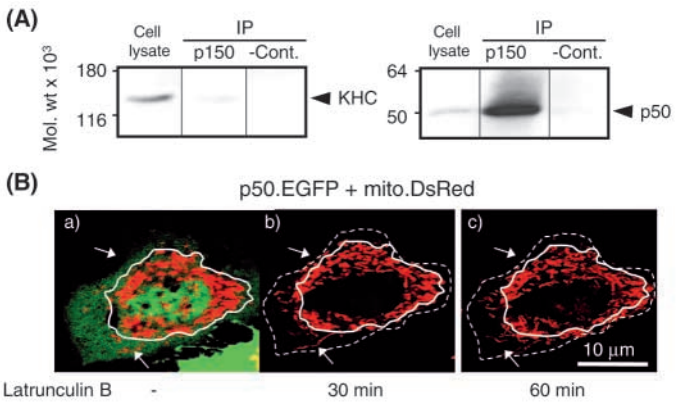

Fig. 5. Kinesin I heavy chain and dynactin complex interact in HeLa cell extract. (A) $p150^{Glued}$ was precipitated from HeLa cell extracts by a monoclonal antibody and blots were probed with a monoclonal anti-kinesin-heavy-chain antibody (SUK4) right panel) or a monoclonal anti-p50 antibody (left panel). Control samples (-Cont.) were precipitated by an unrelated monoclonal antibody. Five μg of protein were loaded from the cell homogenate; the equivalent to 35 μg protein was used as starting material for immunoprecipitation and an equal amount of protein was loaded from the immunoprecipitated samples (lanes $p150^{Glued}$ and -Cont.). (B) Depolymerisation of actin filaments partially restores the normal distribution of mitochondria in p50-expressing cells. Cells were co-transfected with 0.5 μg mito.DsRed and 1 μg p50.EGFP. Twenty hours after transfection cells were incubated with latrunculin B (25 μg ml^{-1}) in KRH buffer at 37°C and then imaged on an Ultra*VIEW*™ Live Cell Confocal Imaging system. Mitochondria of the same cell (a) before the addition of latrunculin B, (b) after a 30-minute incubation or (c) after a 60 minute-incubation with the drug.

Interaction between dynactin and Drp1

The above data suggest that the dynein/dynactin complex is

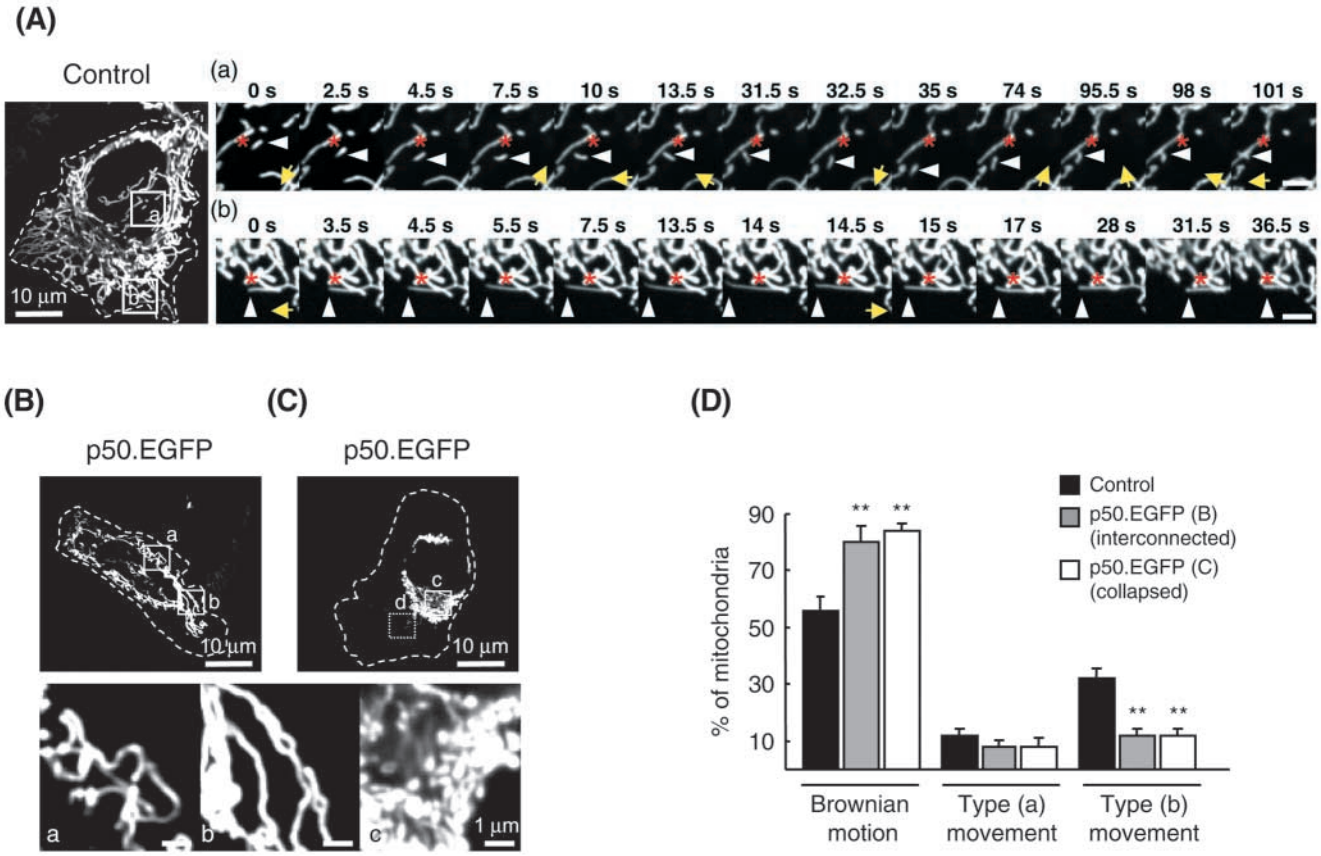

Fig. 6. Mitochondrial movements in live HeLa cells. Cells were co-transfected with 0.25 µg mito.DsRed and (A) 1 µg padTrack-CMV or (B,C) p50.EGFP. Twelve hours after transfection, cells were imaged on an Ultra*VIEW*^{TM} Live Cell Confocal Imaging system in KRH buffer at 37°C; images were acquired at 2 Hz. Boxed regions on the control cell (A) are enlarged in panels a and b. Indicated by the white arrowheads is a single moving mitochondrion whose original starting position is labeled with a red asterisk. Direction of movement is indicated by yellow arrows. (B,C) Mitochondrial distribution in HeLa cells expressing moderate (B) and high (C) levels of p50.EGFP. Note the long interconnected mitochondria in bottom panels Ba and b, and the collapsed mitochondrial structure in bottom panel Cc. (D) Twenty-five mitochondrial regions were selected in ten control cells (black bars), and in cells with moderate (grey bars) and high (white bars) p50 expression and movements of mitochondria were analysed (see Materials and Methods, and Results). Movements of mitochondria are most apparent on dynamic images (see supplementary material Movies 1-5).

important for the correct targeting of Drp1 to the outer mitochondrial membrane. One probable explanation for this requirement is that Drp1 itself, or Drp1-decorated vesicles, are cargoes for dynein. To test this possibility we immunoprecipitated p50, p150^{Glued} and Drp1 from HeLa cells in the presence and absence of detergent (±SP40) and then probed these samples with anti-p50, p150^{Glued} or Drp1 antibodies. A protein band corresponding to p150^{Glued} was observed in the Drp1-immunoprecipitated samples in the absence and presence of detergent (Fig. 9A,B) but was not detected in control samples (Fig. 9A,B). As expected, p150^{Glued} was also present in the samples immunoprecipitated with an anti-p50 antibody (Fig. 9A,B). The amount of p150^{Glued} detected in the anti-Drp1 immunoprecipitated sample was reduced by ~50% in p50 over-expressing cells (Fig. 9B. lane Drp1*). By contrast, over-expressinon of Drp1^{K38A} (carrying a point mutation in the GTPase domain) did not change the amount of p150^{Glued} pulled down with p50 (Fig. 9B, lane p50*). A weak protein band corresponding to p50 was also detected in the anti-Drp1 immunoprecipitated sample only in the absence of detergent (Fig. 9C, panel –pNP40). When immunoprecipitation was carried out with antibodies against the dynactin subunits the Drp1 antibody recognised many strong nonspecific immunoglobulin bands (between 60-80 kDa) and thus the protein corresponding to Drp1 could not be clearly identified. The above data suggest that Drp1 interacts with dynactin and that this interaction is reduced following p50 overexpression.

Discussion

Role of p50 in the control of mitochondrial distribution

The principal aim of these studies was to determine whether the retrograde motor protein, cytoplasmic dynein, is involved in the control of mitochondrial structure in cells. Unexpectedly, we show that interference with the function of cytoplasmic dynein/dynactin complex leads to the displacement of mitochondria towards the nucleus of fibroblasts, a shift more consistent with the inhibition of an anterograde motor (Fig. 2). Although the effect of p50 here was apparently more marked than that described in a earlier study (Burkhardt et al., 1997), close inspection of the data from these authors does indicate some redistribution of mitochondria towards the nucleus

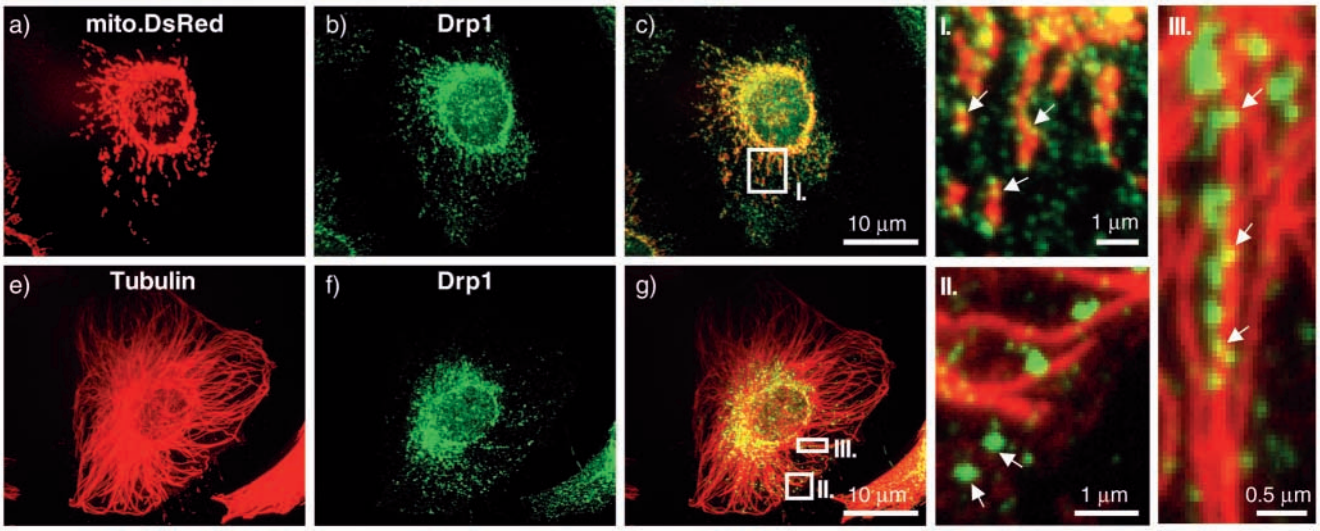

Fig. 7. Subcellular localisation of endogenous Drp1 in HeLa cells. HeLa cells were first fixed with cold methanol-acetone (1:1) and endogenous Drp1 and tubulin were detected by immunofluorescence with an anti-Drp1 (1:250) and an anti-α-tubulin (1:1000) antidody. (a) mito.DsRed; (b,f) Drp1; and (e) α-tubulin-immunofluorescence; (c,g) overlay of a and b, and e and f, respectively. Boxed areas in c and g are shown on an expanded scale in I, and II and III respectively. the enlarged image (III) was rotated 90° clockwise. Arrows indicate Drp1 association with punctate vesicular structures that are aligned along mitochondria (I) and microtubules (II,III).

suggesting that lower levels of p50 overexpression were achieved in the earlier study.

By what mechanisms does the inhibition of a (–)-end-directed motor protein lead to an apparent reduction in anterograde movement of mitochondria? One possible explanation is that disruption of the dynein function also inhibits the activity of kinesin(s) such that the position of the mitochondria is determined largely by actin-based motility. Several studies have reported similar phenomena, i.e. that treatments expected to impair (–)-end motion can also affect (+)-end-directed transport. For example, in extruded squid axoplasm, blockade of the interaction between dynein and dynactin resulted in the inhibition of vesicle transport along microtubules in both directions (Waterman-Storer et al., 1997). Similarly, disruption of kinesin, or dynactin function in squid axoplasm inhibited both retrograde and anterograde transport (Martin et al., 1999). Moreover, complete inactivation of cytoplasmic dynein in mammalian fibroblasts abolished bidirectional motion of lipid droplets (Valetti et al., 1999). Likewise, dynein and dynactin mutations blocked the (+)-end-directed motion of lipid droplets even more strongly than (–)-end motion in *Drosophila* embryos (Gross et al., 2002). Finally, two recent studies showed interdependent roles of kinesin and dynein in *Drosophila* oogenesis and polar transport (Duncan and Warrior, 2002; Januschke et al., 2002; Cohen, 2002).

The existence of such cooperative regulation of kinesin and dynein activities suggests that both motors may be components of the same complex. Indeed, a recent study revealed that dynactin binds to kinesin II and regulates anterograde movement of *Xenopus* melanosomes (Deacon et al., 2003). However, in contrast to the above studies, we found that (a) only a very small proportion of kinesin I interacted with $p150^{Glued}$ in HeLa cells (Fig. 5A); (b) that actin depolymerisation partially reversed the mitochondrial aggregation provoked by p50-overexpression in a small fraction of cells (Fig. 5B) and active outward movements of mitochondria could be observed even at high p50 expression (Movie 5 in supplementary material). Thus, it seems unlikely that the effect of p50 overexpression on mitochondrial morphology is due principally, or even in large part, to the simultaneous inhibition of (+) and (–)-end motors, but that other, less direct mechanisms, must be involved.

Role of p50 in the control of mitochondrial morphology

In addition to the ‘collapsed mitochondria’ phenotype observed by light microscopy, electron microscopy revealed that p50 overexpression led to marked changes in mitochondrial morphology, including the formation of both very long and highly branched structures (Fig. 3). This observation implies that a decrease in the rate of fission versus fusion of mitochondria occurs under these conditions. One possibility is that the enhanced fusion results simply from the greater density of mitochondria in the perinuclear region. However, in mammalian cells (Pitts et al., 1999; Karbowski and Youle, 2003), as in yeast (Karbowski and Youle, 2003), the balance of mitochondrial fission and fusion appears to be carefully controlled by a number of specific remodelling factors, including, dynamin-related protein (Drp1) (Karbowski and Youle, 2003), such that a simple ‘concentration-dependent’ of mitochondrial number is unlikely.

In agreement with previous reports (Yoon et al., 1998; Smirnova et al., 2001) we found here that endogenous Drp1 associates with small, punctate structures that largely align along microtubules (Yoon et al., 1998) and with mitochondria (Yoon et al., 1998; Smirnova et al., 2001) (Fig. 7). Some of these punctate structures also associated with other organelles (Fig. 7) possibly including the ER (Yoon et al., 1998) and peroxisomes (Li and Gould, 2003). Overexpression of p50 caused Drp1 to translocate from these membrane-associated structures, giving a distribution more suggestive of a cytoplasmic localisation (Fig. 8A). Consistent with this, the amount of Drp1 on isolated mitochondria was significantly reduced in p50-overexpressing

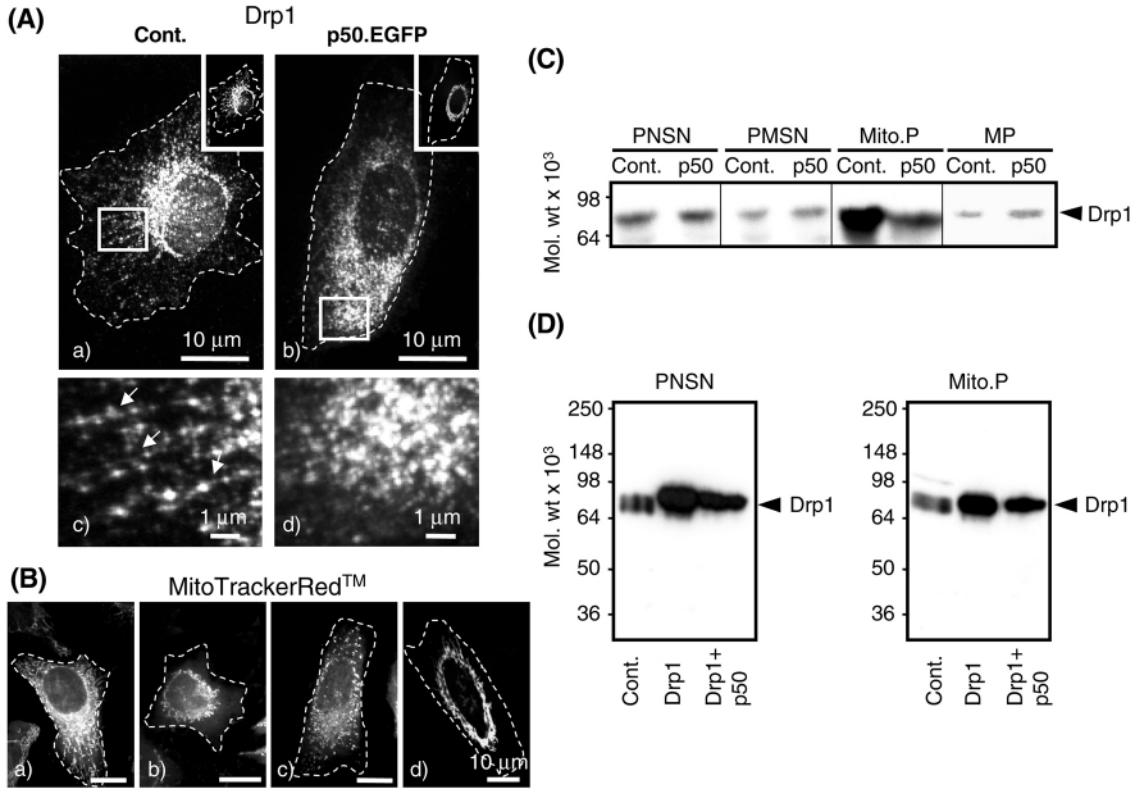

Fig. 8. Overexpression of p50 alters Drp1 localisation to mitochondrial membranes. (A) Endogenous Drp1 was stained in (a) empty vector or (b) p50.EGFP-transfected cells (*n*=15 cells in three independent experiments). Boxed areas in are shown on an expanded scale below (c,d); image in right upper corner shows the distribution of mitochondria in the same cells. Notice the filamentous and dispersed staining of Drp1 in the images of control and in p50 cells. (B) Overexpression of wild-type Drp1 restores normal distribution of mitochondria in p50 cells. Mitochondria were visualised with MitoTrackerRed^{TM} in cells transfected with (a) empty vector, (b) p50.EGFP, (c) p50.EGFP+Drp1^{wt} and (d) Drp1^{K38A} (*n*=8 cells in three independent experiments). Hatched boundaries, obtained from an overlay with the transmitted image of the cell, indicate the cell periphery. Bars, 10 μm (C) Overexpression of p50 reduces the amount of Drp1 on mitochondrial membranes. Cells transfected with p50.EGFP (p50) or empty vector (Cont.) were fractionated as described in Materials and Methods. The post-nuclear supernatant (PNSN), post-mitochondrial supernatant (PMSN), mitochondrial pellet (Mito.P) and microsomal pellet (MP) were probed with a rabbit polyclonal anti-human Drp1 antibody. An equal amount of protein (26 μg/lane) was loaded from each fraction. The antibody recognised Drp1 at the expected size (80 kDa). (D) Overexpression of wild-type Drp1 restores the normal amount of Drp1 on mitochondrial membranes in p50-expressing cells. Post-nuclear supernatant (PNSN) and the mitochondrial pellet (Mito.P) were prepared from control cells (Cont.) and from cells overexpressing Drp1 (Drp1) and Drp1+p50 (Drp1+p50). An equal amount of protein (16 μg) was loaded in each lane. The blots were scanned and quantified with NIH ImageJ software (http://rsb.info.nih.gov/ij/).

cells (Fig. 8C). Intriguingly, point mutations within the GTP-binding domains of Drp1 (K38A and D231N) have previously been shown to alter the distribution of Drp1, and to cause the formation of large cytoplasmic aggregates (Drp1^{K38A}) or diffuse cytosolic (Drp1^{D231N}) staining (Pitts et al., 1999). Moreover, both of the above Drp1 mutants produced long tubular mitochondria collapsed into the perinuclear region (Smirnova et al., 1998; Pitts et al., 1999) (Fig. 8B,d), a strikingly similar phenotype observed following p50 overexpression. Strongly suggesting that the effects of p50 overexpression observed in the present study were due in large part to the translocation of Drp1 from mitochondria, near-normal mitochondrial distribution was restored to p50 over-expressing cells after the introduction of Drp1 (Fig. 8B,c,D).

The present data thus suggest that the dynein/dynactin complex is important for the correct targeting of Drp1 to the outer mitochondrial membrane. One likely explanation for this requirement is that Drp1 itself, or Drp1-decorated vesicles, are cargoes for dynein. The localisation of Drp1-positive structures to microtubules (Fig. 7), which exhibit unidirectional movements from the cell periphery towards the perinuclear region on microtubule tracks in living cells (Yoon et al., 1998), and the fact that Drp1 interacts with the dynactin complex (Fig. 9) strongly support these possibilities. Conversely, microtubule depolymerisation with nocodazole did not significantly affect mitochondrial morphology (Fig. 1B), although it is possible that this manoeuvre, by inhibiting transport of Drp1 both to and from the mitochondrial surface, may have little net effect on association of Drp1 with mitochondria in these short-term (<2 hours) experiments. Another possible explanation for the mistargeting of Drp1 following disruption of dynactin function is that dynactin acts as a receptor for Drp1 on the mitochondrial outer membrane, independently of dynein or microtubules. However, this mechanism would seem unlikely given that the microinjection of a function-blocking anti-dynein antibody (Fig. 4A,B) resulted in the same relocalisation of mitochondria as did p50 overexpression (Fig. 2). Furthermore, the subcellular distribution of dynein on organelles has been shown

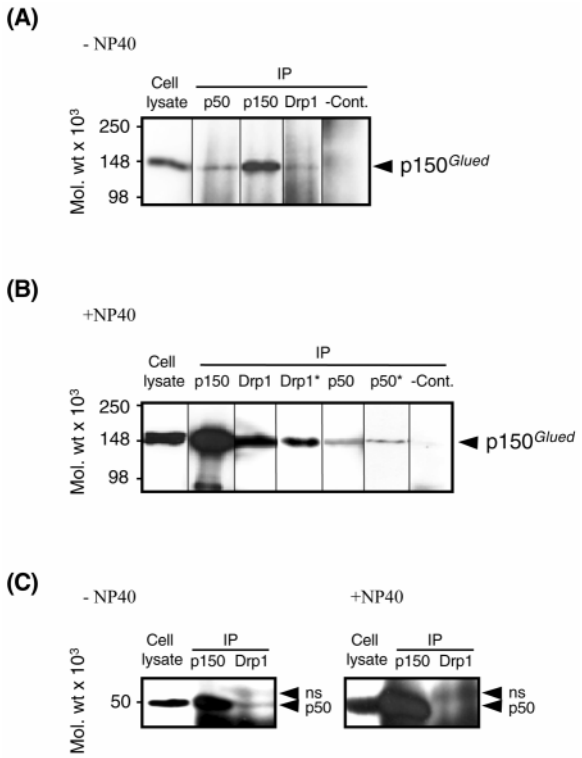

Fig. 9. The Drp1-dynactin complex interacts in HeLa cell extracts. p50, p150^{Glued} and Drp1 were immunoprecipitated (IP) from HeLa cell extracts using the corresponding antibodies. Immunoprecipitations were performed in the presence (+NP40) and absence (-NP40) of detergent. Blots were probed with a monoclonal anti-p150^{Glued} antibody (A,B) or a monoclonal anti-p50 antibody (C). Control samples (-Cont.), precipitated by an unrelated monoclonal antibody or rabbit pre-immune serum. Five μg of protein were loaded from the cell homogenate, and 500 μl were used as starting material for immunoprecipitation. Within each panel, an equal amount of protein was loaded from the immunoprecipitated samples (lanes p150^{Glued} and -Cont.). Drp1*, cells expressing p50; p50*, cells expressing Drp1^{K38A}.

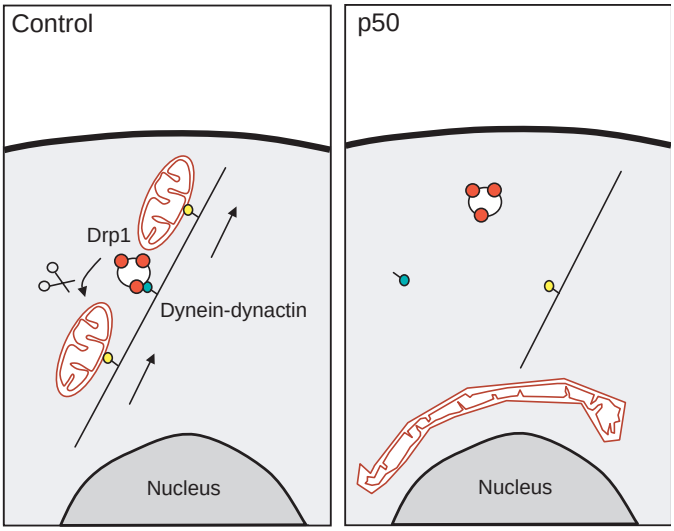

Fig. 10. Possible interaction of Drp1 (red) and dynein-dynactin complexes (green) with microtubules and mitochondria. Efficient fission of mitochondria (Control) facilitate transport of these organelles by anterograde motors including kinesin (yellow). Disruption of dynein-dynactin (p50) leads to the loss of Drp1 from mitochondria, which become more interconnected and consequently a poorer substrate for anterograde transport.

to mirror that of dynactin, suggesting that dynein and dynactin are usually bound together on membrane surfaces (Haberman et al., 2000). Conversely, changes in mitochondrial membrane potential ($\Delta\psi_{mit}$) (Legros et al., 2002; Ishihara et al., 2003), which have been shown to regulate mitochondrial morphology, do not appear to underlie the effect of p50 overexpression because $\Delta\psi_{mit}$ (Fig. 4D) and intramitochondrial [ATP] (not shown) were unaltered in p50 over-expressing cells. Finally, it is conceivable that the mitochondrial network might form a perinuclear cluster as part of a general mechanism to dispose of errant organelles, because other defects of the mitochondrial outer membrane also cause mitochondria to cluster at the cell nucleus (Yano et al., 1997).

Weighing the above evidence, we suspect that the action of p50 is most likely via a shift in the balance between mitochondrial fission and fusion, resulting from a blockade of dynein-dependent Drp1 transport to the mitochondrial outer membrane. As a result, mitochondria become more interconnected and thus become a poorer substrate for anterograde motors, most probably kinesin family members (Fig. 10). Whether motor-protein-dependent recruitment of fission factors to intracellular membranes represents a general mechanism for regulating organellar morphology is, thus, an exciting possibility and will require further investigation.

G.A.R. was supported by Wellcome Trust Programme Grant 067081/Z/02/Z and a Wellcome Trust Research Leave Fellowship. V.C. was supported by NIH grants DK55183 and DK63443, JDRFI Research Grant 197009, and a Network Grant from The Larry L. Hillblom Foundation. Electron microscopy and imaging analysis was performed at The National Center for Microscopy and Imaging Research (UCSD), supported by NIH grant RR04050 to Mark H. Ellisman. We thank Mark Jepson and Alan Leard of the Bristol MRC Imaging Facility for technical assistance, and Professor Peter Cullen for the use of the Ultra*View* confocal microscope.

References

Ainscow, E. K., Zhao, C. and Rutter, G. A. (2000). Acute overexpression of lactate dehydrogenase-A perturbs β-cell mitochondrial metabolism and insulin secretion. *Diabetes* **49**, 1149-1155.

Allan, V. J. and Schroer, T. A. (1999). Membrane motors. *Curr. Opin. Cell Biol.* **11**, 476-482.

Bleazard, W., McCaffery, J. M., King, E. J., Bale, S., Mozdy, A., Tieu, Q., Nunnari, J. and Shaw, J. M. (1999). The dynamin-related GTPase Dnm1 regulates mitochondrial fission in yeast. *Nat. Cell Biol.* **5**, 298-304.

Burkhardt, J. K., Echeverri, C. J., Nilsson, T. and Vallee, R. B. (1997). Overexpression of the dynamitin (p50) subunit of the dynactin complex disrupts dynein-dependent maintenance of membrane organelle distribution. *J. Cell Biol.* **139**, 469-484.

Cohen, R. S. (2002). Oocyte patterning: Dynein and Kinesin. *Curr. Biol.* **12**, R797-R799.

Collins, T. J. and Bootman, M. D. (2003). Mitochondria are morphologically heterogeneous within cells. *J. Exp. Biol.* **206**, 1993-2000.

Collins, T. J., Berridge, M. J., Lipp, P. and Bootman, M. D. (2002). Mitochondria are morphologically and functionally heterogeneous within cells. *EMBO J.* **21**, 1616-1627.

Deacon, S. W., Serpinskaya, A. S., Vaughan, P. S., Fanarraga, M. L.,

Vernos, I., Vaughan, K. T. and Gelfand, V. I. (2003). Dynactin is required for bidirectional organelle transport. *J. Cell Biol.* **160**, 297-301.

Duncan, J. E. and Warrior, R. (2002). The cytoplasmic Dynein and Kinesin motors have interdependent roles in patterning the Drosophila oocyte. *Curr. Biol.* **12**, 1982-1991.

Echeverri, C. J., Paschal, B. M., Vaughan, K. T. and Vallee, R. B. (1996). Molecular characterization of the 50-kD subunit of dynactin reveals function for the complex in chromosome alignment and spindle organization during mitosis. *J. Cell Biol.* **132**, 617-633.

Gill, S. R., Schroer, T. A., Szilak, I., Steuer, E. R., Sheetz, M. P. and Cleveland, D. W. (1991). Dynactin, a conserved, ubiquitously expressed component of an activator of vesicle motility mediated by cytoplasmic dynein. *J. Cell Biol.* **115**, 1639-1650.

Gross, S. P., Welte, M. A., Block, S. M. and Wieschaus, E. F. (2002). Coordination of opposite-polarity microtubule motors. *J. Cell Biol.* **156**, 715-724.

Habermann, A., Schroer, T. A., Griffiths, G. and Burkhardt, J. K. (2001). Immunolocalization of cytoplasmic dynein and dynactin subunits in cultured macrophages: enrichment on early endocytic organelles. *J. Cell Sci.* **114**, 229-240.

He, T.-C., Zhou, S., DaCosta, L. T., Yu, J., Kinzler, K. W. and Vogelstein, B. (1998). A simplified system for generating recombinant adenoviruses. *Proc. Natl. Acad. Sci. USA* **95**, 2509-2514.

Heald, R., Tournebize, R., Blank, T., Sandaltzopoulos, R., Becker, P., Hyman, A. and Karsenti, E. (1996). Self-organization of microtubules into bipolar spindles around artificial chromosomes in Xenopus egg extracts. *Nature* **382**, 420-425.

Helfand, B. T., Mikami, A., Vallee, R. B. and Goldman, R. D. (2002). A requirement for cytoplasmic dynein and dynactin in intermediate filament network assembly and organization. *J. Cell Biol.* **157**, 795-806.

Hirokawa, N. (1998). Kinesin and dynein superfamily proteins and the mechanism of organelle transport. *Science* **279**, 519-526.

Holleran, E. A., Karki, S. and Holzbaur, E. L. (1998). The role of the dynactin complex in intracellular motility. *Int. Rev. Cytol.* **182**, 69-109.

Ishihara, N., Jofuku, A., Eura, Y. and Mihara, K. (2003). Regulation of mitochondrial morphology by membrane potential, and DRP1-dependent division and FZO1-dependent fusion reaction in mammalian cells. *Biochem. Biophys. Res. Commun.* **301**, 891-898.

Januschke, J., Gervais, L., Dass, S., Kaltschmidt, J. A., Lopez-Schier, H., Johnston, D. S., Brand, A. H., Roth, S. and Guichet, A. (2002). Polar transport in the Drosophila oocyte requires Dynein and Kinesin I cooperation. *Curr. Biol.* **12**, 1971-1981.

Jouaville, L. S., Pinton, P., Bastianutto, C., Rutter, G. A. and Rizzuto, R. (1999). Regulation of mitochondrial ATP synthesis by calcium: evidence for long-term metabolic priming. *Proc. Nat. Acad. Sci. USA* **96**, 13807-13812.

Karbowski, M. and Youle, R. J. (2003). Dynamics and mitochondrial morphology in healthy cells and during apoptosis. *Cell Death Differ.* **10**, 870-880.

Karbowski, M., Spodnik, J. H., Teranishi, M., Wozniak, M., Nishizawa, Y., Usukura, J. and Wakabayashi, T. (2001). Opposite effects of microtubule-stabilizing and microtubule-destabilizing drugs on biogenesis of mitochondria in mammalian cells. *J. Cell Sci.* **114**, 281-291.

Knowles, M. K., Guenza, M. G., Capaldi, R. A. and Marcus, A. H. (2002). Cytoskeletal-assisted dynamics of the mitochondrial reticulum in living cells. *Proc. Nat. Acad. Sci. USA* **99**, 14772-14777.

Krylyshkina, O., Kaverina, I., Kranewitter, W., Steffen, W., Alonso, M. C., Cross, R. A. and Small, J. V. (2002). Modulation of substrate adhesion dynamics via microtubule targeting requires kinesin-1. *J. Cell Biol.* **156**, 349-359.

Lee, S. S. and Banting G. (2002). Characterisation of the lumenal domain of TGN38 and effects of elevated expression of TGN38 on glycoprotein secretion. *Eur. J. Cell Biol.* **81**, 609-621.

Legros, F., Lombes, A., Frachon, P. and Rojo, M. (2002). Mitochondrial fusion in human cells is efficient, requires the inner membrane potential, and is mediated by mitofusins. *Mol. Biol. Cell* **13**, 4343-4354.

Li, X. and Gould, S. J. (2003). The dynamin-like GTPase DLP1 is essential for peroxisome division and is recruited to peroxisomes in part by PEX11. *J. Biol. Chem.* **278**, 17012-17020.

Martin, M., Iyadurai, S. J., Gassman, A., Gindhart, J. G., Hays, T. S. and Saxton, W. M. (1999). Cytoplasmic dynein, the dynactin complex, and kinesin are interdependent and essential for fast axonal transport. *Mol. Biol. Cell* **10**, 3717-3728.

Molnar, E., Varadi, A., McIlhinney, R. A. J. and Ashcroft, S. J. H. (1995). Identification of functional ionotropic glutamate receptor proteins in pancreatic β-cells and in islets of Langerhans. *FEBS Lett.* **371**, 253-257.

Morris, R. L. and Hollenbeck, P. J. (1995). Axonal transport of mitochondria along microtubules and F-actin in living vertebrate neurons. *J. Cell Biol.* **131**, 1315-1326.

Nangaku, M., Sato-Yoshitake, R., Okada, Y., Noda, Y., Takemura, R., Yamazaki, H. and Hirokawa, N. (1994). KIF1B, a novel microtubule plus end-directed monomeric motor protein for transport of mitochondria. *Cell* **79**, 1209-1220.

Newmeyer, D. D. and Ferguson-Miller, S. (2003). Mitochondria: releasing power for life and unleashing the machineries of death. *Cell* **112**, 481-490.

Park, M. K., Ashby, M. C., Erdemli, G., Petersen, O. H. and Tepikin, A. V. (2001). Perinuclear, perigranular and sub-plasmalemmal mitochondria have distinct functions in the regulation of cellular calcium transport. *EMBO J.* **20**, 1863-1874.

Pitts, K. R., Yoon, Y., Krueger, E. W. and McNiven, M. A. (1999). The dynamin-like protein DLP1 is essential for normal distribution and morphology of the endoplasmic reticulum and mitochondria in mammalian cells. *Mol. Biol. Cell* **10**, 4403-4417.

Rappaport, L., Oliviero, P. and Samuel, J. L. (1998). Cytoskeleton and mitochondrial morphology and function. *Mol. Cell Biochem.* **184**, 101-105.

Rizzuto, R., Brini, M., Murgia, M. and Pozzan T. (1993). Microdomains with high Ca^{2+} close to IP3-sensitive channels that are sensed by neighbouring mitochondria. *Science* **262**, 744-747.

Rizzuto, R., Pinton, P., Carrington, W., Fay, F. S., Fogarty, K. E., Lifshitz, L. M., Tuft, R. A. and Pozzan, T. (1998). Close contacts with the endoplasmic reticulum as determinants of mitochondrial Ca^{2+} responses. *Science* **280**, 1763-1766.

Rutter, G. A. and Rizzuto, R. (2000). Regulation of mitochondrial metabolism by ER Ca^{2+} release: an intimate connection. *Trends Biochem. Sci.* **25**, 215-221.

Smirnova, E., Shurland, D. L., Ryazantsev, S. N. and van der Bliek, A. M. (1998). A human dynamin-related protein controls the distribution of mitochondria. *J. Cell Biol.* **143**, 351-358.

Smirnova, E., Griparic, L., Shurland, D. L. and van der Bliek, A. M. (2001). Dynamin-related protein Drp1 is required for mitochondrial division in mammalian cells. *Mol. Biol. Cell* **12**, 2245-2256.

Staubli, W. A. (1963). A new embedding technique for electron microscopy, combining a water-soluble epoxy resin (Durcopan) with water-insoluble araldite. *J. Cell Biol.* **16**, 197-201.

Tanaka, Y., Kanai, Y., Okada, Y., Nonaka, S., Takeda, S., Harada, A. and Hirokawa, N. (1998). Targeted disruption of mouse conventional kinesin heavy chain, kif5B, results in abnormal perinuclear clustering of mitochondria. *Cell* **93**, 1147-1158.

Valetti, C., Wetzel, D. M., Schrader, M., Hasbani, M. J., Gill, S. R., Kreis, T. E. and Schroer, T. A. (1999). Role of dynactin in endocytic traffic: effects of dynamitin overexpression and colocalization with CLIP-170. *Mol. Biol. Cell* **10**, 4107-4120.

Varadi, A. and Rutter, G. A. (2002). Dynamic imaging of endoplasmic reticulum $[Ca^{2+}]$ in MIN6 β-cells using recombinant cameleons: roles of SERCA2 and ryanodine receptors. *Diabetes* **51**, S190-S201.

Varadi, A., Ainscow, E. K. Allan, V. J. and Rutter, G. A. (2002). Involvement of conventional kinesin in glucose-stimulated secretory-granule movements and exocytosis in clonal pancreatic β-cells. *J. Cell Sci.* **115**, 4177-4189.

Varadi, A., Cirulli, V. and Rutter, G. A. (2004). Mitochondrial localisation as a determinant of capacitative Ca^{2+} entry in HeLa cells. *Cell. Calcium* (in press).

Waterman-Storer, C. M., Karki, S. B., Kuznetsov, S. A., Tabb, J. S., Weiss, D. G., Langford, G. M. and Holzbaur, E. L. (1997). The interaction between cytoplasmic dynein and dynactin is required for fast axonal transport. *Proc. Natl. Acad. Sci. USA* **94**, 12180-12185.

Yaffe, M. P. (1999). Dynamic mitochondria. *Nat. Cell Biol.* **1**, E149-E150.

Yano, M., Kanazawa, M., Terada, K., Namchai, C., Yamaizumi, M., Hanson, G., Hoogenraad, N. and Mori, M. (1997). Visualisation of mitochondrial protein import in cultured mammalian cells with green fluorescent protein and effects of overexpression of the human import receptor Tom20. *J. Biol. Chem.* **272**, 8459-8465.

Yoon, Y., Pitts, K. R., Dahan, S. and McNiven, M. A. (1998). A novel dynamin-like protein associates with cytoplasmic vesicles and tubules of the endoplasmic reticulum in mammalian cells. *J. Cell Biol.* **140**, 779-793.

Yoon, Y., Pitts, K. R. and McNiven, M. A. (2001). Mammalian dynamin-like protein DLP1 tubulates membranes. *Mol. Biol. Cell* **12**, 2894-2905.